Texture Based Classification of Malaria Parasites from Giemsa-Stained Thin Blood Films

Suchada Tantisatirapong[*†] and **Wongsakorn Preedanan**[**], Non-members

ABSTRACT

Quantification of parasitaemia is an important part of a microscopic malaria diagnosis. Giemsa-stained thin blood smear is the gold standard method for detecting malaria parasite enumeration. However, manual counting reveals the limitations of human inconsistency and fatigue, as well as the unreliability of accuracy and non-reproducibility. In this paper, the texture-based classification approach is investigated. The methods consist of the following processes: pre-processing, segmentation, feature extraction and the classification of erythrocytes. The preprocessing is applied for image conversion and enhancement. The segmentation combines local adaptive thresholding, morphological process and watershed transform to extract red blood cells, separate touching and overlapping cells. Texture analysis is performed to establish parameters obtained from first-order, second-order and higher-order statistical analysis and wavelet transform. Two feature selection approaches, the sequential forward selection method and sequential backward selection method, integrated with a support vector machine classifier are examined to obtain the optimal feature set for identifying the *Plasmodium falciparum* stages. We found that gray-level co-occurrence matrices based textural features were highly selected. The proposed method produces 98.87% accuracy for binary classification, 99.56% accuracy for ring stage classification, and 99.48% accuracy for tropozoite stage classification.

Keywords: Malaria Parasites, *Plasmodium Falciparum*, Giemsa-Stained Thin Blood Film, Parasitaemia, Segmentation, Texture Analysis, Classification

1. INTRODUCTION

Malaria is a life-threating infectious disease, which is considered the second most common cause of illness and related deaths in the world. The World Malaria Report of 2018 stated that there were an estimated 219 million and 435,000 related deaths in 2017 [1]. Although global malaria control has been delayed, the reduction of global malaria cases has not been significantly reported, especially in South East Asia and Africa. Malaria mortality is mostly caused by *Plasmodium falciparum* (*P.falciparum*), which is the most common and harmful species.

Antimalarial drugs are investigated in research laboratories where drug susceptibility tests are conducted through enumerating infected red blood cells in the asexual erythrocytic stage (percentage parasitaemia). Traditionally, percentage parasitaemia is quantified by manual counting, which is considered to be the gold standard. However, manual counting requires expertise and experience, and results in fatigue, is time-consuming as well as facing unreproducible and unreliable results [2]. Inaccurate percent parasitaemia affects clinical diagnosis and therapeutic procedure. Automated quantification is therefore useful to improve the performance of quantifying parasite density.

In order to improve the process of quantification of percentage parasitaemia, we investigated and implemented an automatic quantification of *P.falciparum* parasite stages based on texture analysis. The proposed system is aimed to assist biological scientists to process the parasite enumeration more accurately and quickly in the laboratory-based research environment.

2. RELATED STUDIES

Giemsa-stained thin blood smear is the gold standard method to enumerate *P. falciparum* stages in the erythrocytic stage [3]. In the new developmental cycle of *P. falciparum*, after reinvasion of the merozoite into new red blood cell (RBC), the parasite developed through ring, trophozoite and schizont stages prior to RBC ruptures for the next cycle. The morphology of the different erythrocytic stages in the Giemsa staining of *P. falciparum* thin smear can be described as follows [4]. Morphology of the ring stages has a ring-like shape. The structured ring

Manuscript received on August 8, 2019 ; revised on October 31, 2019 ; accepted on November 2, 2019. This paper was recommended by Associate Editor Chanon Warisarn.

[*]The author is with the Department of Biomedical Engineering, Faculty of Engineering, Srinakharinwirot University, Thailand.

[**]The author is with the Department of Information and Communications Engineering, Tokyo Institute of Technology, Japan.

[†]Corresponding author. E-mail: suchadat@g.swu.ac.th

Digital Object Identifier 10.37936/ecti-eec.2020181.208115

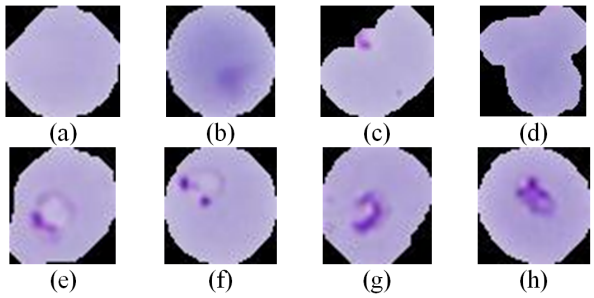

Fig.1: *Normal erythrocyte (a), stained on normal erythrocytes (b,c), touching and overlapping cells (d), P.falciparum ring (e,f), P.falciparum trophozoite (g,h).*

is delicate cytoplasm and 1 to 2 ring head(s) indicated by chromatin dots. The trophozoite stage has an irregular shape with compact cytoplasm. It has more complex structure and is larger in size than the ring stages. The schizont stage contains various numbers of merozoite, depending on the ages of the parasites. The parasite cell becomes larger and occupies about two-thirds of the RBC. Hemozoin, a brown pigment, is a product from hemoglobin digestion and can be detected from the trophozoite to the schizont stage. The enumeration of RBC number and each parasite stages can be confounded by stained artifacts, such as stain residual, cell debris, hemozoin and pyknotic (dead parasites) containing RBC. Moreover, overlapped RBCs cannot be separately counted as individual cells. Examples of normal RBC, RBC with stain, *P.falciparum* ring and trophozoite are illustrated in Fig. 1.

Studies of automated determination for *P.falciparum* on thin blood film smears are found in terms of binary and multi-stage classification. The binary classification reports the differentiation of normal and infected cells. In the multi-stage classification, the parasites in ring, trophozoite, schizont and gametocyte stages are commonly reported.

Automated parasitaemia quantification software named 'MalariaCount' was proposed by S.W.S. Sio et al. [5]. After an input image is selected, the software initially enhances an image using an adaptive histogram equalization method. Erythrocyte are preliminarily segmented using an edge detection and edge-linking methods, following clump splitting method to separate connected and overlapped cells. Differentiation of normal and infected cells is identified using binary morphology and edge correlation coefficient.

Y. Purwar et al. [6] proposed the automated algorithm to count RBC and identify malaria parasites. The Giemsa-stained thin blood smear image is firstly enhanced using local histogram equalization. Erythrocytes are sequentially extracted using the Chan-Vese segmentation method, while stained particles are examined based on intensity value.

Fully automated binary classification of malaria parasites was presented by S.S. Savkare et al. [7]. Otsu's threshold based segmentation was applied to extract RBC, while watershed transform based segmentation was used to separate overlapped and connected cells. The features of erythrocytes were derived from a gray-level histogram and a saturated histogram, before feeding to the SVM binary classifiers. The RBF kernel function based SVM gave higher detection rate than the polynomial and linear kernel functions based SVM.

A multi-stage malaria (ring, trophozoite, schizont forms) classification system was presented by G. Diaz et al. [8]. Initially, an input image is enhanced using local low-pass filter. Cells are then segmented using the RGB color space and inclusion-tree representation approaches, while cell contours are extracted using the clump splitting method. Cell features are derived from combined techniques: color histogram, saturation level histogram, gray-level histogram, Tamura texture histogram and Sobel histogram. Support vector machines and neural network classifiers are used to evaluate classification accuracy.

F. Boray Tek et.al. [9] proposed a processing pipeline to extract the stained structures, determine the infected species and identify life-cycle stages of malaria parasites. The stained objects were extracted from plotting pixel distributions in RGB space histograms. The features of extracted images were quantified using color histogram, local area granulometry and shape measurements, after various pre-processing steps including image non-uniform illumination correction, scale normalization, and color correction. The features were given to the multi-classifiers comparing with the three different models. Although their proposed method was good, this work was validated with a limited data set.

Previously, the authors proposed the framework of automated detection of malaria parasites in Giemsa-stained thin blood films [10]. Firstly, we used local adaptive thresholding to separate the erythrocyte from the background image. Morphological opening and watershed transform were used in order to remove small artifacts and separate connected cells, respectively. The first-order statistics texture analysis was applied to extract the textural features from each segmented cells and investigated the best combined feature set. The features were given to the SVMs binary classifier based on linear and RBF kernel functions to identify erythrocytes as normal or infected cells. We computed only first-order statistics based texture analysis.

As aforementioned, erythrocyte features for malaria parasite detection in thin blood smear images illustrated various combined feature sets based on morphological, texture and intensity properties [11]. In this paper, we aim to investigate the distinct feature combination based on first, second and

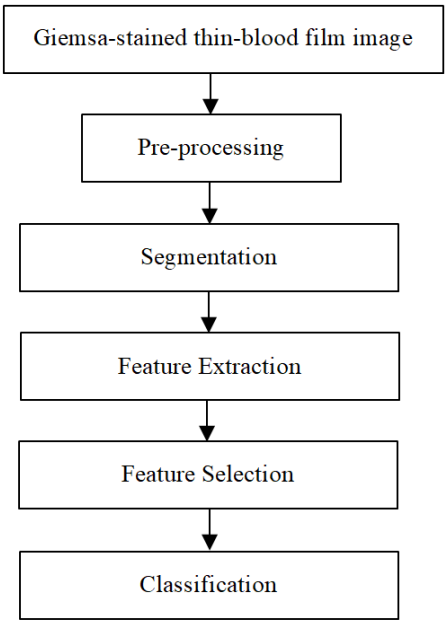

Fig.2: *Overview of the texture based classification of malaria parasites from Giemsa-stained thin blood films.*

higher-order statistical analysis as well as wavelet transforms, in order to classify *P.falciparum* ring and trophozoite forms.

3. MATERIAL AND METHODS

3.1 Image Acquisition

The image acquisition of Giemsa-stained thin blood films was conducted using an Olympus BX51 microscope equipped with an Olympus DP71 digital camera and DP controller software version v3.2.1.276. The acquired images were taken with the resolution of 1360-by-1024 pixels and recorded in JPEG file format. In this work, we used 340 images: 60 images for training and 280 images for testing.

3.2 Pre-Processing

The image quality is affected by various factors such as dye duration, Giemsa-stained intensity and residuals. Although the thin blood film images were taken in the same environment, the images still have a dynamic range of luminous intensity and distribution depending on smear preparation. In order to prepare an input image, image enhancement is applied using a 3×3 median filter to smoothen and reduce noise of a grayscale image converted from a colour Giemsa-stained thin blood film image. An overview of the proposed method is illustrated in Fig. 2.

3.3 Segmentation

Segmentation is applied to obtain individual erythrocyte extracted from thin blood film image background. Commonly, the challenges faced in cell segmentation are separation of connected and overlapped cells, which is hard to manage during smear preparation. We combined well-known methods based on local adaptive thresholding, morphology and watershed to separate erythrocytes by taking the touching and overlapping conditions into account.

Firstly, a grayscale image is converted to a binary image using a local adaptive thresholding method [12], which adaptively adjusts the threshold according to local neighbourhood intensity to identify the foreground and background. In the binary image, the holes in cells and Giemsa-stained residuals are filled and removed using a morphological opening operator, including an erosion and dilation process. In addition, connected and overlapped cells are separated using watershed transform, prior to labelling matrix of individual cells.

3.4 Feature Extraction

Feature extraction is the process to represent the identity of infected erythrocytes in each stage. Texture analysis is performed to establish parameters such as statistical analysis, wavelet transform, gray-level co-occurrence matrix, and gray-level run length matrix. First-order statistical analysis including mean, standard deviation, skewness and kurtosis [13], are calculated from a gray-level histogram of each cell in an image.

Gray-Level Co-occurrence Matrices (GLCM) is a second-order statistical analysis, considering the relations between pixel pairs across the entire intensity range of gray levels. The method tabulates a matrix of a number of pixel occurrences in the same intensity range in four directions, which are 0, 45, 90 and 135 degrees at a specified distance. In this experiment, we converted a grayscale image into 2 sizes of GLCMs which are 8×8 GLCM and 32×32 GLCM with a distance of one. After creating a GLCM, we extracted 18 statistical values from the derived matrices [14–16].

Gray-Level Run Length Matrices (GLRLM) is a higher-order statistical analysis. This method is defined by specifying directions which are 0, 45, 90 and 135 degrees and then counting the occurrence of runs for each gray level and length in those directions. We converted a grayscale image into 2 matrix sizes like GLCM and computed 11 statistical values from these matrices [17–18].

In transform-based texture analysis, two-dimensional (2D) wavelet transform is applied to decompose segmented erythrocyte image at defined level. We employed 3 types of wavelet transforms, Haar, Daubechies 2 and Symlet 4. Corresponding energy is then derived from the transform matrices.

3.5 Feature Selection

As a large number of textural features are generated from each cell, an appropriate feature set is required to reduce the data dimensionality and improve the classification outcome. The feature selection method named Minimum Redundancy and Maximum Relevance (mRMR) [19] is applied to grade the correlation degree of each feature to the class. The mRMR method is a feature selection based on the mutual information technique that removes the redundant subsets and selects parameters dominantly related with the class. We used this method to select the top-ten most relevant features. Subsequently, the selected features are given to the SVM classifier and optimized by using Sequential Forward Selection (SFS) and Sequential Backward Selection (SBS) methods. The evaluation was performed using the leave-one-out cross-validation technique.

The SFS method starts with an empty feature set in the model. Then it repeatedly adds relevant features to the model until no features increase the classification outcome. The SBS method starts with the top-ten most relevant features in the model. Then, it repeatedly removes less relevant features from the model until the best feature combination provides the highest classification accuracy.

3.6 Classification

The Support Vector Machine (SVM) is a supervised learning classification model that can provide various kernel functions to suit with different data types. The SVM computes the maximum marginal separation line from a set of training data to separate two classes. By using a kernel function, it maps the original features into higher dimensional space where it computes a hyperplane that maximises the distance from the hyperplane to the training data in each class. The SVM predicts unlabelled test data by mapping it into the feature space to indicate the side of the separating plane where the test data lays.

In this work, the SVM is applied to identify erythrocytes as normal cells, infected cells in the ring stage and in the trophozoite stage. The linear and radial basis function (RBF) kernels are investigated and the evaluation is examined using the leave-one-out cross validation method.

4. EXPERIMENTAL RESULTS AND DISCUSSION

We examined the proposed method with the Giemsa-stained thin blood films of 340 images, divided into 60 training and 280 test images. The training data contains a total of 12,667 erythrocytes, 182 infected erythrocytes in ring stage and 149 infected erythrocytes in trophozoite stage. The test data contains a total of 54,154 erythrocytes, 1,003 infected erythrocytes in ring stage and 393 infected erythrocytes in trophozoite stage.

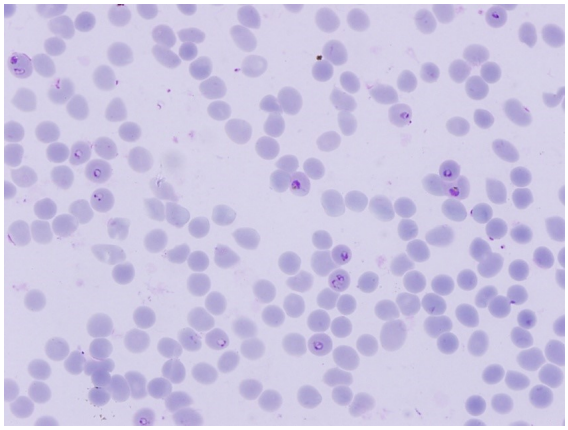

Fig.3: *Giemsa-stained thin blood film image of Plasmodium falciparum.*

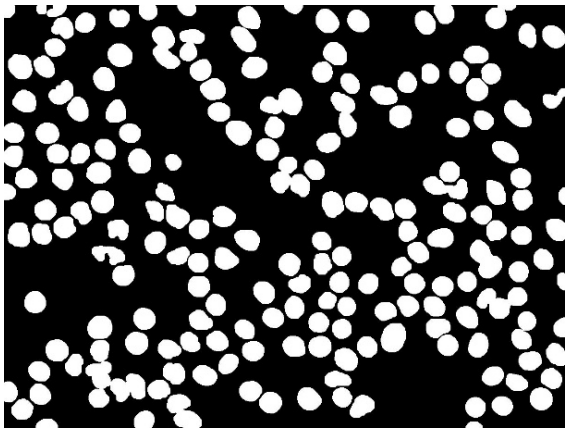

Fig.4: *An example of segmented erythrocyte image.*

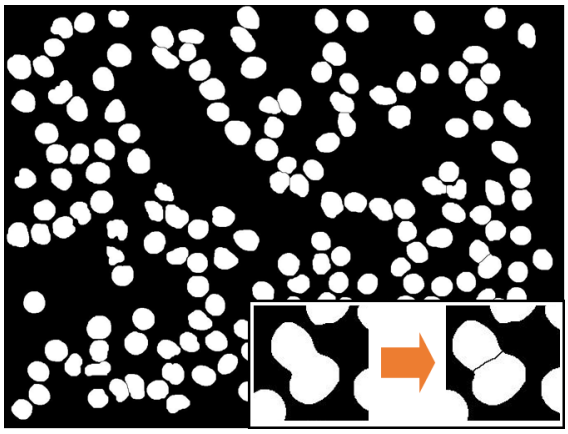

Fig.5: *Separation of overlapped cells processed by watershed transform method.*

In the pre-processing, RGB images of Giemsa-stain thin blood films (Fig. 3) were converted to gray-scale images and smoothened using a median filter. Erythrocytes are extracted using local adaptive thresh-

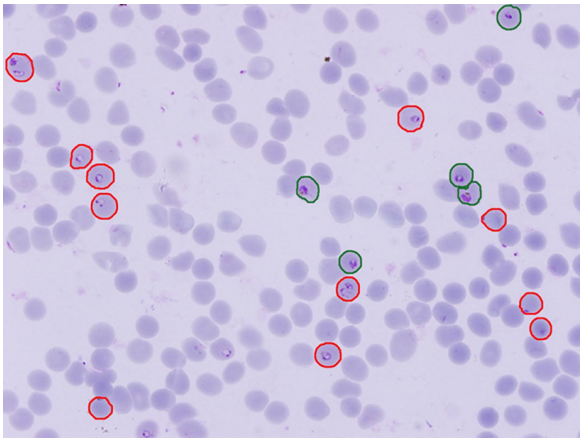

Fig.6: *The result classification of malaria parasites image (red contours show ring stage and green contours show trophozoite stage).*

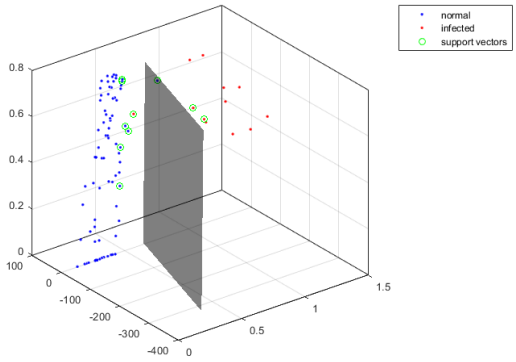

Fig.7: *Linear kernel function based SVM classification of normal and infected blood cells.*

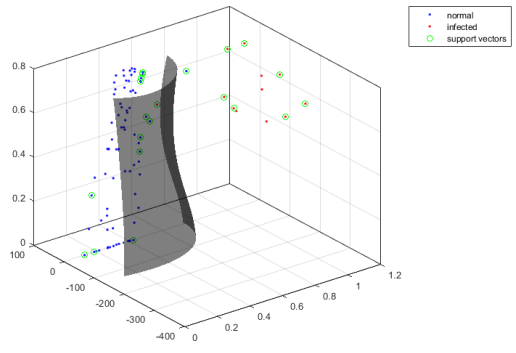

Fig.8: *RBF kernel function based SVM classification of normal and infected blood cells.*

olding and morphological opening. Connected and overlapped cells are separated by using watershed transform method as shown in Figs. 4 and 5.

After cells are extracted, textural features derived from statistical analysis and wavelet transform are

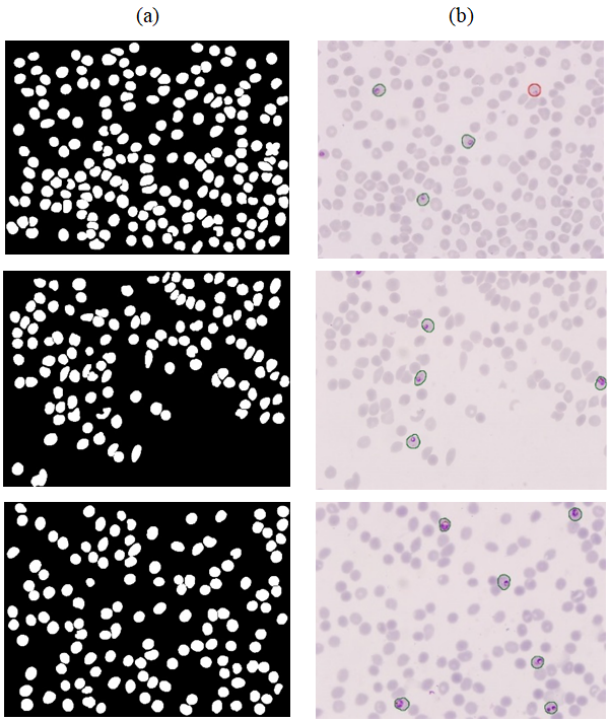

Fig.9: *Example results of texture based classification of Plasmodium falciparum from Giemsa-stained thin blood films. Column (a) segmented Giemsa-stained thin blood film image of Plasmodium falciparum. Column (b) classification results of malaria parasites image (red contours show ring stage and green contours show trophozoite stage).*

generated for each individual cell. These textural features are subsequently given to the mRMR method for selecting the ten top features (Table 1). An optimal combined feature set is obtained from the two techniques, i.e. the SFS and SBS methods, both given to the SVM classifier (Table 1). Example classification results are shown in Figs. 6 and 9. The linear and RBF kernel functions based SVM are used to investigate classification accuracy as shown in Figs. 7 and 8, respectively. The graphical user interface of the proposed system is implemented to delineate the infected cells and report the total number of cells, percentage parasitaemia, percentage *P.falciparum* ring and percentage *P.falciparum* trophozoite as shown in Fig. 10.

In Table 1, the GLCM based features are the prominent feature type selected from the mRMR method. The optimal feature set obtained from the SFS method contained fewer members than that from the SBS method. However, there are some commonly selected features by both SFS and SBS methods: difference entropy, dissimilarity and information measure of the correlation2, which are derived from the GLCM. These textural features can reveal the dissimilarity of surface texture between normal and infected erythrocytes more vividly than the other textural features.

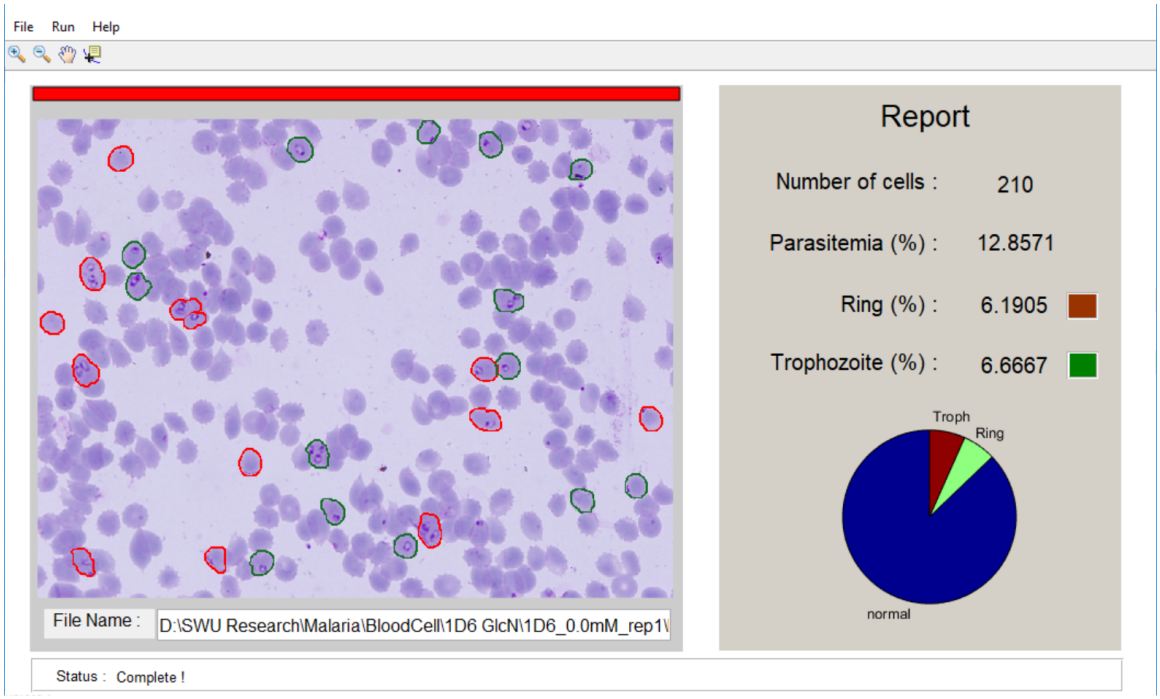

Fig.10: *Graphic User Interface of texture based classification for Plasmodium Stained Thin blood flims.*

Table 1: *Selected features from mRMR method, sequential forward selection and sequential backward selection.*

Features	Sequential Forward Selection		Sequential Backward Selection	
	Linear	RBF	Linear	RBF
Cluster Shade (GLCM $32 \times 32, 45°$)			✓	✓
Contrast (GLCM $8 \times 8, 0°$)			✓	
Difference entropy (GLCM $32 \times 32, 0°$)	✓	✓		✓
Difference entropy (GLCM $32 \times 32, 90°$)			✓	✓
Contrast (GLCM $8 \times 8, 45°$)			✓	✓
Dissimilarity (GLCM $32 \times 32, 90°$)	✓		✓	✓
Contrast (GLCM $32 \times 32, 135°$)			✓	✓
Difference entropy (GLCM $32 \times 32, 135°$)			✓	✓
Difference variance (GLCM $32 \times 32, 45°$)			✓	✓
Information measure of correlation2 (GLCM $8 \times 8, 45°$)	✓	✓	✓	✓

In general, in Tables 2 and 3, the features selected from the SFS with a linear kernel function based SVM classifier tend to produce higher accuracy for binary, ring form and trophozoite classification. However, in Table 4, features selected from the SBS with RBF kernel function based SVM classifier provide higher results for binary, ring form and trophozoite classification. From Tables 2, 3 and 4, RBF kernel function tended to give better results than linear kernel function for sensitivity rates. The highest classification accuracy for binary, ring form and trophozoite are 98.87%, 99.56% and 99.48%, respectively. From the results, we can conclude that our frameworks can produce sensitivity, specificity and accuracy as high as other works.

GLCM based textural features are highly selected by the feature selection method. This shows that the second-order statistics based texture analysis presents higher discrimination between normal and infected *P.falciparum* cells. This is because the GLCM can quantify the surface property more comprehensively and distinctively than the first and higher-order statistics based texture analysis as well as wavelet transform. However, computing GLCM involves pre-defined parameters which can affect texture property: distance of paired pixels and number of gray level intensity, should be taken into consideration for optimal outcome. Compared to our previous work [20], the GLCM-based texture analysis yielded better average accuracy that the fuzzy inference system. This shows that GLCM based textural features provided promising characteristics for malaria parasites detection.

The *P.falciparum* stage classification outcome depends on various factors. The characteristics of blood smear images such as a large number of overlapped cells and stained residuals from manual blood smear

Table 2: *The classification results of binary, ring stage and trophozoite stage classification based on the features selected from the mRMR method.*

Classification	Sensitivity(%)		Specificity(%)		Accuracy(%)	
	Linear	RBF	Linear	RBF	Linear	RBF
Binary	96.13	97.15	94.93	88.90	94.94	89.08
Ring	80.37	91.19	96.98	89.24	98.84	89.14
Trophozoite	58.15	90.57	99.43	99.38	96.32	99.27

Table 3: *The classification results of binary, ring stage and trophozoite stage classification based on the features selected from sequential forward selection.*

Classification	Sensitivity(%)		Specificity(%)		Accuracy(%)	
	Linear	RBF	Linear	RBF	Linear	RBF
Binary	92.99	96.97	98.22	97.57	98.87	97.56
Ring	76.03	86.10	98.45	97.07	98.40	99.56
Trophozoite	51.83	95.30	99.69	99.62	99.01	96.82

Table 4: *The classification results of binary, ring stage and trophozoite stage classification based on the features selected from sequential backward selection.*

Classification	Sensitivity(%)		Specificity(%)		Accuracy(%)	
	Linear	RBF	Linear	RBF	Linear	RBF
Binary	92.37	97.95	93.15	97.81	93.11	97.83
Ring	89.33	94.20	97.87	97.72	97.55	97.59
Trophozoite	65.23	88.34	90.02	99.65	89.67	99.48

preparation, can lead to inaccurate cell segmentation. Giemsa-stained residual attached on normal cells can appear like parasites. These parasites appear as infected cells in the ring stage. Infected cells with multiple heads in the ring stage can also be misclassified as an infected cell in a trophozoite stage.

5. CONCLUSION

This paper presented the texture-based classification of *Plasmodium falciparum* parasites stages. The textural features of segmented gray-scale erythrocytes are derived from statistical analysis and wavelet transform. The mRMR based feature selection combined with sequential forward selection or sequential backward selection are applied to select an optimal feature set prior being given to the SVM classifier. We found that gray-level co-occurrence matrices based texture analysis is the dominant method, compared to the first-order and higher-order statistics as well as wavelet transform.

The optimal feature set selected by the sequential forward selection yields lesser number of features and tends to give higher accuracy than the feature set selected by the sequential backward selection. The proposed method produces 98.87% accuracy for binary classification, 99.56% accuracy for ring stage classification, and 99.48% accuracy for tropozoite stage classification.

ACKNOWLEDGEMENT

We are thankful to Dr. Aiyada Aroonsri from the National Center for Genetic Engineering and Biotechnology (BIOTEC) for providing insightful suggestions and dataset. We also would like to thank Pargorn Puttapirat, an undergraduate students at Srinakharinwirot University for assisting in the experiment.

References

[1] World Health Organization, "World Malaria Report 2018," WHO Press, Geneva, Switzerland, 2018.

[2] P. Puttapirat, M. Phothisonothai and S. Tantisatirapong, "Automated segmentation of erythrocytes from Giemsa-stained thin blood films," in *Proceeding of 8th International Conference on Knowledge and Smart Technology*, Chiangmai, Thailand, pp. 219–223, 2016.

[3] B. Malleret, C. Claser, A. S. M. Ong, R. Suwanarusk, K. Sriprawat, S. W. Howland, B. Russell, F. Nosten, L. Rénia, "A rapid and robust tri-color flow cytometry assay for monitoring malaria parasite development," *Scientific Reports*, vol. 1, pp. 118, 2011.

[4] K. Silamut, N. H. Phu, C. Whitty, G. D. H. Turner, K. Louwrier, N.T.H. Mai, J. A. Simpson, T. T. Hien, N. J. White, "A quantitative analysis of the microvascular sequestration of malaria parasites in the human brain", *The American Journal of Pathology, American Society for Investigative Pathology*, vol. 115, no. 2, pp. 395–410, 1999.

[5] S. W. S. Sio, W. Sun, S. Kumar, W. Z. Bin, S. S. Tan, S. H. Ong, H. Kikuchi, Y. Oshima and K. S. W. Tan, "MalariaCount: an image analysis-based program for the accurate determination of parasitaemia," *Journal of Microbiological Methods*, vol. 68, pp. 11–18, 2007.

[6] Y. Purwar, S. L. Shah, G. Clarke, A. Almugairi and A. Muehlenbachs, "Automated and unsupervised detection of malarial parasites in microscopic images," *Malaria Journal*, vol. 10, pp. 364, 2011.

[7] S. S. Savkare and S. P. Narote, "Automatic system for classification of erythrocyte infected with malaria and identification of parasite's life stage", *Procedia Technology*, vol. 6, pp. 405–410, 2012.

[8] G. Díaz, F. A. González, and E. Romero, "A semi-automatic method for quantification and classification of erythrocytes infected with malaria parasites in microscopic images," *Journal of Biomedical Informatics*, vol. 42, pp. 296–307, 2009.

[9] F. B. Tek, A. G. Dempster , I. Kale, "Parasite detection and identification for automated thin blood film malaria diagnosis," *Computer Vision and Image Understanding*, vol. 114, pp. 21–32, 2010.

[10] W. Preedanan, M. Phothisonothai, W. Senavongse, and S. Tantisatirapong, "Automated detection of plasmodium from Giemsa-stained thin blood films," in *Proceeding of 8th International Conference on Knowledge and Smart Technology*, Chiangmai, Thailand, pp. 215–218, 2016.

[11] S. S. Devi, S. A. Sheikh, and R. H. Laskar, "Erythrocyte Features for Malaria Parasite Detection in Microscopic Images of Thin Blood Smear: A Review," *International Journal of Interactive Multimedia and Artificial Intelligence*, vol. 4, no. 2, pp. 34–39, 2016.

[12] G. Xiong (2020). Local Adaptive Thresholding MATLAB Central [Online]. Available: `http://www.mathworks.com/matlabcentral/fileexchange/8647-local-adaptive-thresholding`, MATLAB Central File Exchange.

[13] F. Malik and B. Baharudin, "The statistical quantized histogram texture features analysis for image retrieval based on median and laplacian filters in the DCT domain," *The International Arab Journal of Information Technology*, vol. 10, no. 6, pp. 616–624, 2013.

[14] R. M. Haralick, K. Shanmugam and I. Dinstein, "Textural features of image classification," *IEEE Transactions on Systems, Man and Cybernetics*, vol. SMC-3, no. 6, pp. 610–621, 1973.

[15] L. Soh and C. Tsatsoulis, "Texture analysis of SAR sea ice imagery using gray level co-occurrence matrices," *IEEE Transactions on Geoscience and Remote Sensing*, vol. 37, no. 2, pp. 780–795, 1999.

[16] D. A. Clausi, "An analysis of co-occurrence texture statistics as a function of grey level quantization," *Canadian Journal of Remote Sensing*, vol. 28, no. 1, pp. 45–62, 2002.

[17] X. Tang, "Texture information in run-length Matrices," *IEEE Transactions on Image Processing*, vol. 7, no. 11, pp. 1602–1609,1998.

[18] X. Wei, Gray Level Run Length Matrices Toolbox v1.0, Software, Beijing Aeronautical Technology Research Center, 2007.

[19] H. Peng, L. Fuhui and C. Ding, "Feature selection based on mutual information: criteria of max-dependency, max-relevance, and min-redundancy," *IEEE Transactions on Pattern Analysis and Machine Intelligence*, vol. 27, no. 8, pp. 1226–1238, 2005.

[20] S. Tantisatirapong and M. Phothisonothai, "Classification of in vitro blood stages of plasmodium falciparum based on fuzzy interference system," in *Proceeding of 10th International Conference on Knowledge and Smart Technology (KST)*, Chiang Mai, Thailand, pp. 293-296, 2018.

Suchada Tantisatirapong received B.Eng. (Computer Engineering), M.Eng.Sc. (Biomedical Engineering) and Ph.D. (Biomedical Engineering) from National University of Singapore, Singapore, University of New South Wales, Australia and University of Birmingham, United Kingdom in 2006, 2007 and 2015. She is currently an assistant professor in the Department of Biomedical Engineering, Faculty of Engineering, and Srinakharinwirot University, Thailand. Her research interests are in the area of biomedical image and signal processing as well as human-machine interaction applications.

Wongsakorn Preedanan received B. Eng. (Biomedical Engineering), and M.Eng. (Information and Communication for Embedded Systems) from Srinakharinwirot University, Thailand and Sirindhorn International Institute of Technology, Thammasat University, Thailand in 2016 and 2018. He is currently a Ph.D. student in the Department of Information and Communications Engineering, Tokyo Institute of Technology, Japan. His research interests are in the area of biomedical image processing and deep learning.